Psychological Medicine (2017), **47**, 1637–1646. © Cambridge University Press 2017
doi:10.1017/S0033291717000101

ORIGINAL ARTICLE

Selective functional disconnection of the orbitofrontal subregions in schizophrenia

Y. Xu[1,2]†, W. Qin[1]†, C. Zhuo[3]†, L. Xu[1], J. Zhu[1], X. Liu[1] and C. Yu[1]*

[1] *Department of Radiology, Tianjin Key Laboratory of Functional Imaging, Tianjin Medical University General Hospital, Tianjin, China*
[2] *Department of Computed Tomography and Magnetic Resonance Imaging, Handan First Hospital, Handan, Hebei, China*
[3] *Tianjin Anning Hospital, Tianjin, China*

Background. As a disconnection syndrome, schizophrenia has shown impaired resting-state functional connectivity (rsFC) in the orbitofrontal cortex (OFC); however, the OFC is a rather heterogeneous region and the rsFC changes in the OFC subregions remain unknown.

Method. A total of 98 schizophrenia patients and 102 healthy controls underwent resting-state functional MRI using a sensitivity-encoded spiral-in imaging sequence (SENSE-SPIRAL) to reduce susceptibility-induced signal loss and distortion. The OFC subregions were defined according to a previous parcellation study that divided the OFC into the anterior (OFCa), medial (OFCm), posterior (OFCp), intermediate (OFCi), and lateral (OFCl) subregions. The rsFC was compared using two-way repeated-measures ANOVA.

Results. Whether or not global signal regression, compared with healthy controls, schizophrenia patients consistently exhibited decreased rsFC between the left OFCi and the left middle temporal gyrus and the right middle frontal gyrus (MFG), between the right OFCi and the right MFG and the left inferior frontal gyrus, between the right OFCm and the middle cingulate cortex and the left Rolandic operculum. These rsFC changes still remained significant even after cortical atrophy correction.

Conclusions. These findings suggest a selective functional disconnection of the OFC subregions in schizophrenia, and provide more precise information about the functional disconnections of the OFC in this disorder.

Received 6 November 2015; Revised 4 January 2017; Accepted 5 January 2017; First published online 10 February 2017

Key words: Magnetic resonance imaging, orbitofrontal subregions, resting-state functional connectivity, schizophrenia, sensitivity-encoded spiral-in imaging sequence.

Introduction

Schizophrenia is a devastating and disabling neuropsychiatric disorder. The neural mechanisms of this disorder have been attributed to structural and functional abnormalities of the brain (Ellison-Wright *et al.* 2008; Andreasen, 2010; Andreasen *et al.* 2011; Chan *et al.* 2011; Asami *et al.* 2012; Liu *et al.* 2016). The orbitofrontal cortex (OFC) has been implicated in multiple functions, including sensory integration and reward learning, cognitive flexibility, control of emotion, decision making, social behavior and mnemonic functions (Zald & Kim, 1996; Kringelbach & Rolls, 2004; Kringelbach, 2005). Most of these functions are impaired in schizophrenia (Mandal *et al.* 1998; Mullen *et al.* 2000; Kester *et al.* 2006; Shad *et al.* 2007), which has been ascribed to the structural and functional deficits in the OFC in schizophrenia (Naudts & Hodgins, 2006; Sapara *et al.* 2007; Baas *et al.* 2008; Dolan & Fullam, 2009).

The human OFC is a rather heterogeneous region and can be further divided into several subregions based on the features in cytoarchitecture and connection (Ongur *et al.* 2003; Mackey & Petrides, 2010; Kahnt *et al.* 2012), which may account for functional diversity of the OFC (Zald & Kim, 1996; Kringelbach & Rolls, 2004; Kringelbach, 2005). Disconnection has been considered as an important feature of schizophrenia (Pettersson-Yeo *et al.* 2011). Several studies have suggested the reduction in the resting-state functional connectivity (rsFC) of the OFC in schizophrenia (Lynall *et al.* 2010; Hoptman *et al.* 2014; Pu *et al.* 2014). However, these studies have regarded the OFC as a single region, leaving the rsFC changes in the OFC subregions in schizophrenia largely unknown. The more precise information may improve our understanding of the role of the OFC in the physiopathology of schizophrenia.

In previous functional magnetic resonance imaging (fMRI) studies of the OFC, the use of the echo planar

* Address for correspondence: Professor C. Yu., Department of Radiology, Tianjin Medical University General Hospital, No. 154, Anshan Road, Heping District, Tianjin 300052, China.
(Email: chunshuiyu@vip.163.com)
† These authors contributed equally to this work.

https://doi.org/10.1017/S0033291717000101 Published online by Cambridge University Press

imaging (EPI) sequence to acquire imaging data is technically problematic because this sequence would inevitably introduce imaging signal dropout, geometric distortion, and susceptibility artifacts in the OFC region, which may lower our confidence in interpreting our findings. To reduce susceptibility artifacts in air/tissue interfaces, a sensitivity-encoded spiral imaging (SENSE-SPIRAL) technique has been proposed to acquire fMRI data (Pruessmann *et al.* 1999; Truong & Song, 2008). This technique can improve the functional imaging quality of the OFC and make the rsFC analysis of the OFC more reliable than the EPI sequence.

In this study, we used the SENSE-SPIRAL technique to acquire the resting-state fMRI data to investigate the rsFC changes of the OFC subregions in schizophrenia. The OFC subregions were defined according to a previous parcellation study of the OFC based on the structural imaging (Liu *et al.* 2015*b*). Two potential influential factors were also considered: the effect of cortical atrophy and the effect of the global signal regression (GSR) (Yang *et al.* 2014).

Materials and method

Participants

A total of 98 right-handed schizophrenia patients and 102 sex-, age- and handedness-matched healthy controls were recruited in this study. Diagnoses for schizophrenia patients were confirmed using the Structured Clinical Interview for DSM-IV. All the participants were aged from 18 to 55 years. Exclusion criteria for all participants were MRI contraindications, poor image quality, presence of a systemic medical illness or CNS disorder, history of head trauma, and lifetime history of substance abuse (determined by self-report of participants). Additional exclusion criteria for healthy controls were history of any Axis I or II disorders, a psychotic disorder and first-degree relative with a psychotic disorder. The Positive and Negative Syndrome Scale (PANSS; Kay *et al.* 1987) was used to quantify the clinical symptoms of schizophrenia patients. This study was approved by the Medical Research Ethics Committee of Tianjin Medical University General Hospital, and all participants provided written informed consent.

Imaging data acquisition

MRI was performed using a 3.0-T MR system (Discovery MR750, General Electric, USA). Tight but comfortable foam padding was used to minimize head motion, and earplugs were used to reduce scanner noise. Sagittal 3D.

T1-weighted images were acquired by a brain volume sequence with the following scan parameters: repetition time (TR) = 8.2 ms; echo time (TE) = 3.2 ms; inversion time = 450 ms; flip angle (FA) = 12°; field of view (FOV) = 256 mm × 256 mm; matrix = 256 × 256; slice thickness = 1 mm, no gap; and 188 sagittal slices. Two sets of resting-state fMRI data were acquired. A gradient-echo single-shot EPI sequence was performed with the following parameters: TR/TE = 2000/45 ms; FOV = 220 mm × 220 mm; matrix = 64 × 64; FA = 90°; slice thickness = 4 mm; gap = 0.5 mm; 32 interleaved transverse slices; 180 volumes. A SENSE-SPIRAL sequence was performed with the following parameters: TR/TE = 1400/30 ms; FA = 60°, acceleration factor = 2. The FOV, matrix, slice thickness, gap, and slice number were the same as the EPI sequence. During these fMRI scans, all subjects were instructed to keep their eyes closed, to relax and move as little as possible, to think of nothing in particular, and to not fall asleep.

Definition of OFC subregions

The OFC subregions for the rsFC analysis were defined according to a previous parcellation study of the OFC based on the artifact-free structural imaging (Liu *et al.* 2015*b*). The human OFC was parcellated into 10 symmetrical subregions, including the anterior (OFCa), medial (OFCm), posterior (OFCp), intermediate (OFCi), and lateral (OFCl) subregions in each hemisphere (Supplementary Fig. S1).

Image quality assessments

Image quality of the OFC was compared between the EPI and SENSE-SPIRAL sequences, including the relative signal intensity (rSI), distortion, signal-to-noise ratio (SNR), and variance coefficient of the signal intensity. The specific methods are provided in Supplementary Material and the results are show in Supplementary Table S1 and Supplementary Figs S2–S4. Although the SENSE-SPIRAL sequence had lower SNR, this sequence showed less distortion, higher rSI and lower variance coefficient of SI in several OFC subregions than the EPI sequence. These results indicate that the SENSE-SPIRAL sequence is more suitable for imaging the OFC than the EPI sequence. To further exclude the possible effect of signal loss on our results, we excluded subjects whose rSI in any OFC subregion was <0.5.

Gray-matter volume (GMV) calculation

The GMV of each voxel was calculated using Statistical Parametric Mapping software (SPM8; http://www.fil.ion.ucl.ac.uk/spm/software/spm8/). The structural MR

https://doi.org/10.1017/S0033291717000101 Published online by Cambridge University Press

images were segmented into gray matter (GM), white matter and cerebrospinal fluid using the standard unified segmentation model. After an initial affine registration of GM concentration map into the Montreal Neurological Institute (MNI) space, GM concentration images were nonlinearly warped using diffeomorphic anatomical registration through the exponentiated Lie algebra (DARTEL) technique (Ashburner, 2007) and were resampled to 1.5-mm cubic voxels. The GMV of each voxel was obtained by multiplying GM concentration map by the nonlinear determinants derived from the spatial normalization step. Finally, GMV images were smoothed with a Gaussian kernel of $6 \times 6 \times 6$ mm^3 full-width at half maximum (FWHM). After spatial preprocessing, the normalized, modulated, and smoothed GMV maps were used for statistical analysis.

fMRI data preprocessing

The two sets of resting-state fMRI data were preprocessed using SPM8 with the same procedures. The resting-state fMRI data were preprocessed in the following steps. The first 10 volumes from each subject were discarded to allow the signal to reach equilibrium and to allow the participant to adapt to the scanning noise. The remaining 240 volumes were corrected for the acquisition time delay between slices. Rigid realignment was then performed to estimate and correct for the motion displacement. Three schizophrenia patients were excluded because of excessive head motion; the remaining subjects' fMRI data were within the defined head motion thresholds (translational or rotational motion parameters lower than 2 mm or 2°). We also calculated frame-wise displacement (FD), which indexes the volume-to-volume changes in head position (Power *et al.* 2013). There was no significant difference in mean FD ($t = 0.16$, $p = 0.872$) between schizophrenia patients and healthy controls. Then nuisance covariates were regressed out from the motion corrected fMRI data, including the mean signals of whole brain, white matter and cerebrospinal fluid, six rigid motion parameters and their first-level derivatives, linear trends, and spike volumes that had FD >0.5. Because some recent studies suggested that the results without GSR may differ from the results with GSR in schizophrenia (Yang *et al.* 2014), both the results with and without GSR were reported. The datasets were band-pass filtered with a frequency range of 0.01–0.08 Hz. A two-step co-registration method was used to transform the regressed fMRI data into the MNI space. First, the mean realigned fMRI images were affinely (12 parameters) co-registered with individual structural images; then the structural images were affinely (12 parameters) co-registered with the standard MNI T1-weighted template. The generated parameters for these two co-registration steps were used to normalize the regressed fMRI data. The normalized fMRI data were resampled into a voxel size of $3 \times 3 \times 3$ mm^3. Finally, the normalized fMRI volumes were smoothed with a Gaussian kernel of $6 \times 6 \times 6$ mm^3 FWHM.

The rsFC patterns of OFC subregions

After OFC subregions were normalized to the MNI space, we conducted seed-based rsFC analysis with the following procedures. For each individual dataset, Pearson's correlation coefficients between the mean time series of each seed and time series of each voxel in other parts of the brain were computed and converted to z values using Fisher's r-to-z transformation to improve the normality (Liu *et al.* 2015*a*). To show rsFC pattern of each OFC subregion, individuals' z values of each seed were separately entered into a one-sample t test in a voxel-wise manner using SPM8. A false discovery rate (FDR) correction with $p < 0.05/10 = 0.005$ was used to identify brain regions that showed significant positive correlations with each OFC subregion. The negative correlations may be caused by GSR, and they might not reflect true neural activity (Weissenbacher *et al.* 2009). To avoid misleading readers, we only focused on positive correlations. We used paired t tests to compare voxel-wise connectivity differences between every two of OFC subregions (FDR correction). Because we only interested in connectivity differences between OFC subregions at the same hemisphere, the paired t test was applied to the left and right OFC subregions, respectively. To account for these additional 20 comparisons, we used a FDR-corrected p value of $0.05/20 = 0.0025$ to correct for multiple comparisons.

We also generated fingerprints to quantitatively show connectivity differences across OFC subregions. The detailed methods are provided in the Supplementary material. We designed a bootstrap analysis to verify the consistency of these connectivity patterns over subjects. For each OFC subregion, we performed resampling 1000 times, and then computed the mean overlap ratio and standard deviation of its connectivity maps. Moreover, to test the effect of distance factor to the connectivity pattern, we reconstructed these connectivity maps by multiplying the square root of Euclidian distance for each OFC subregion.

Intergroup rsFC differences of OFC subregions

We identified brain regions that are positively correlated with OFC subregions in schizophrenia patients and healthy controls, respectively. We then transformed these connectivity maps into binary masks. For each

https://doi.org/10.1017/S0033291717000101 Published online by Cambridge University Press

OFC subregion, the connectivity mask from patients and that from controls were merged into one union mask. In this union mask, each voxel was significantly correlated with the OFC subregion at least in one of two populations. This union mask was used to define the spatial range for intergroup comparisons. For GSR data, after controlling for the effects of age and gender, we performed voxel-wise intergroup comparisons using two-way repeated measures ANOVA with diagnostic group and OFC subregion as two factors. We only focused on the group × subregion interaction effect ($p < 0.05$, FDR correction). If there were significant interactions, *post-hoc* analysis were performed to identify specific OFC subregion's connectivity that showed significant intergroup differences ($p < 0.05$, Bonferroni correction).

GMV analysis

We extracted GMV of each OFC subregion and compared between the two groups using a two-sample t test. Multiple comparisons were corrected using the Bonferroni method with a significant threshold of $p < 0.05$.

The effect of GMV atrophy on the rsFC alterations

To test the effect of GMV atrophy on the rsFC alterations of the OFC subregions, we extracted each rsFC of the OFC subregions with significant intergroup differences in the voxel-based analysis. Then we compared intergroup differences in these rsFCs with and without GMV correction.

Correlations between the rsFC alterations and clinical parameters

To test whether rsFCs of the OFC subregions with significant intergroup differences were correlated with clinical variables, we extracted these rsFCs and calculated Spearman's correlation coefficients between these rsFCs and clinical parameters (i.e. PANSS scores, illness duration, and antipsychotic dosage) ($p < 0.05$, uncorrected).

Ethical standards

The authors assert that all procedures contributing to this work comply with the ethical standards of the relevant national and institutional committees on human experimentation and with the Helsinki Declaration of 1975, as revised in 2008.

Results

Demographic and clinical characteristics

After excluding subjects without enough signal intensity in the OFC and those with an excessive head motion, a total of 86 schizophrenia patients and 95 healthy controls were included in the further analysis. The demographic and clinical characteristics of these subjects are shown in Table 1. There were no significant intergroup differences in sex ($\chi^2 = 2.35$, df = 1, $p = 0.126$) and age ($t = 0.22$, df = 179, $p = 0.828$). Eighty-one patients were receiving treatment with one or more atypical antipsychotics, and the remaining five patients had never received any medications.

The rsFC patterns of the OFC subregions

The rsFC maps of the OFC subregions in healthy controls and schizophrenia patients are shown in Fig. 1. There were significant differences in rsFC patterns between any two subregions (Supplementary Fig. S5). The fingerprints showed specific connectivity pattern for each OFC subregion (Supplementary Fig. S6). Here, we only described the main connectivity pattern of each OFC subregion. Both the OFCa and OFCm connected with the posterior cingulate cortex (PCC), anterior cingulate cortex (ACC), and medial prefrontal cortex (MPFC). The OFCa also connected with the angular gyrus (AG). The OFCp connected with the parahippocampus (PH) and temporal pole (TP). The OFCi connected with the inferior frontal gyrus (IFG), middle frontal gyrus (MFG), inferior temporal gyrus (ITG), and inferior parietal lobule (IPL). The OFCl connected with the insular (Ins), IFG, and TP. Bootstrap analysis showed that the mean overlap ratios of each OFC subregion's connectivity were >80% except for the bilateral OFCp (Supplementary Fig. S7). Although distance factor may alter specific connectivity strengths, both voxel-wise connectivity map (Supplementary Fig. S8) and fingerprint (Supplementary Fig. S9) of each OFC subregion showed similar connectivity patterns with original ones when multiplying the square root of Euclidian distance. We overlaid the rsFC maps of schizophrenia patients onto those of healthy controls. We found that both healthy controls and schizophrenia patients exhibited similar rsFC patterns for each OFC subregion (Supplementary Fig. S10). For a specific OFC subregion, the left and right seeds showed similar rsFC patterns.

Intergroup rsFC differences of the OFC subregions with GSR

For GSR data, there were seven brain regions showing significant group × subregion interaction, including the middle cingulate cortex (MCC), the left IFG, MTG and

https://doi.org/10.1017/S0033291717000101 Published online by Cambridge University Press

Table 1. *Demographic and clinical characteristics of schizophrenia patients and healthy controls*

Variables	Patients ($N = 85$)	Controls ($N = 96$)	t/χ^2	p
Age (years)	33.4 ± 7.8	33.1 ± 10.7	$t = 0.22$	0.828[a]
Gender (males/females)	46/40	40/55	$\chi^2 = 2.35$	0.126[b]
Illness duration (months)	118.7 ± 90.2			
PANSS				
Positive subscore	16.6 ± 8.1			
Negative subscore	20.2 ± 8.9			
Current antipsychotic dosage (chlorpromazine equivalents) (mg/d)	469.6 ± 355.3			

N, Number; PANSS, Positive and Negative Syndrome Scale; S.D., standard deviation.
The data are shown as the mean ± S.D.
[a] Two-sample *t* test was used to test the difference in age between the two groups.
[b] χ^2 test was used to test the difference in gender between the two groups.

Rolandic operculum (RO), and the right AG, MFG and MPFC (Fig. 2). *Post-hoc* comparisons are shown in Table 2. In schizophrenia patients, the left OFCi showed significant reduced rsFC with the left MTG and the right MFG. The right OFCi showed reduced rsFC with the left IFG and the right MFG. Both the left OFCl and the bilateral OFCm showed reduced rsFC with the right MPFC. The right OFCm also showed reduced rsFC with the MCC and the left RO.

Intergroup rsFC differences of the OFC subregions without GSR

To test the effect of GSR, we also repeated two-way repeated-measures ANOVA ($p < 0.001$, uncorrected) for fMRI data without GSR. There were seven brain regions showing significant group × subregion interaction, including the MCC, the left IFG, MTG, AG, Ins and RO, and the right MFG (Supplementary Fig. S11).

Consistent rsFC differences of the OFC subregions with and without GSR

Although it is a matter of debate on the correctness of GSR in the rsFC comparisons between schizophrenia patients and healthy controls, we found some consistent findings across the two methods. We overlaid the brain regions showing significant group × subregion interaction with GSR onto those without GSR. From the overlap map, there were five regions consistently showing significant interaction (Supplementary Fig. S12), including the MCC, the left IFG, MTG, RO, and the right MFG.

Volumetric alterations of the OFC subregions

Compared with healthy controls, the schizophrenia patients had significantly reduced GMV ($p < 0.05$, Bonferroni corrected) in all 10 OFC subregions (Supplementary Table S2).

The effect of the GMV on rsFC of the OFC subregions

GMV alterations may affect the results of the rsFC analysis. In order to exclude the effect of the GMV, we repeated the rsFC analysis with GMV correction. Compared with the results without GMV correction, all brain regions showing consistent rsFC reduction also remained statistically significant after GMV correction (Supplementary Table S3).

Correlations between rsFC of the OFC subregions and clinical parameters

In schizophrenia patients, we performed a partial correlation analysis to examine the correlations between these changed rsFCs and clinical parameters (i.e. duration of illness, PANSS positive scores, PANSS negative scores and current antipsychotic dosage in chlorpromazine equivalents). However, we did not find any significant correlations between rsFC alterations and those clinical parameters.

Discussion

In this study, we systematically investigated rsFC changes of the OFC subregions in schizophrenia. We found that three OFC subregions consistently showed decreased functional connectivity, suggesting that the OFC has a selective functional disconnection in schizophrenia.

Method consideration

In contrast with most previous resting-state fMRI studies that acquired data using an EPI sequence,

https://doi.org/10.1017/S0033291717000101 Published online by Cambridge University Press

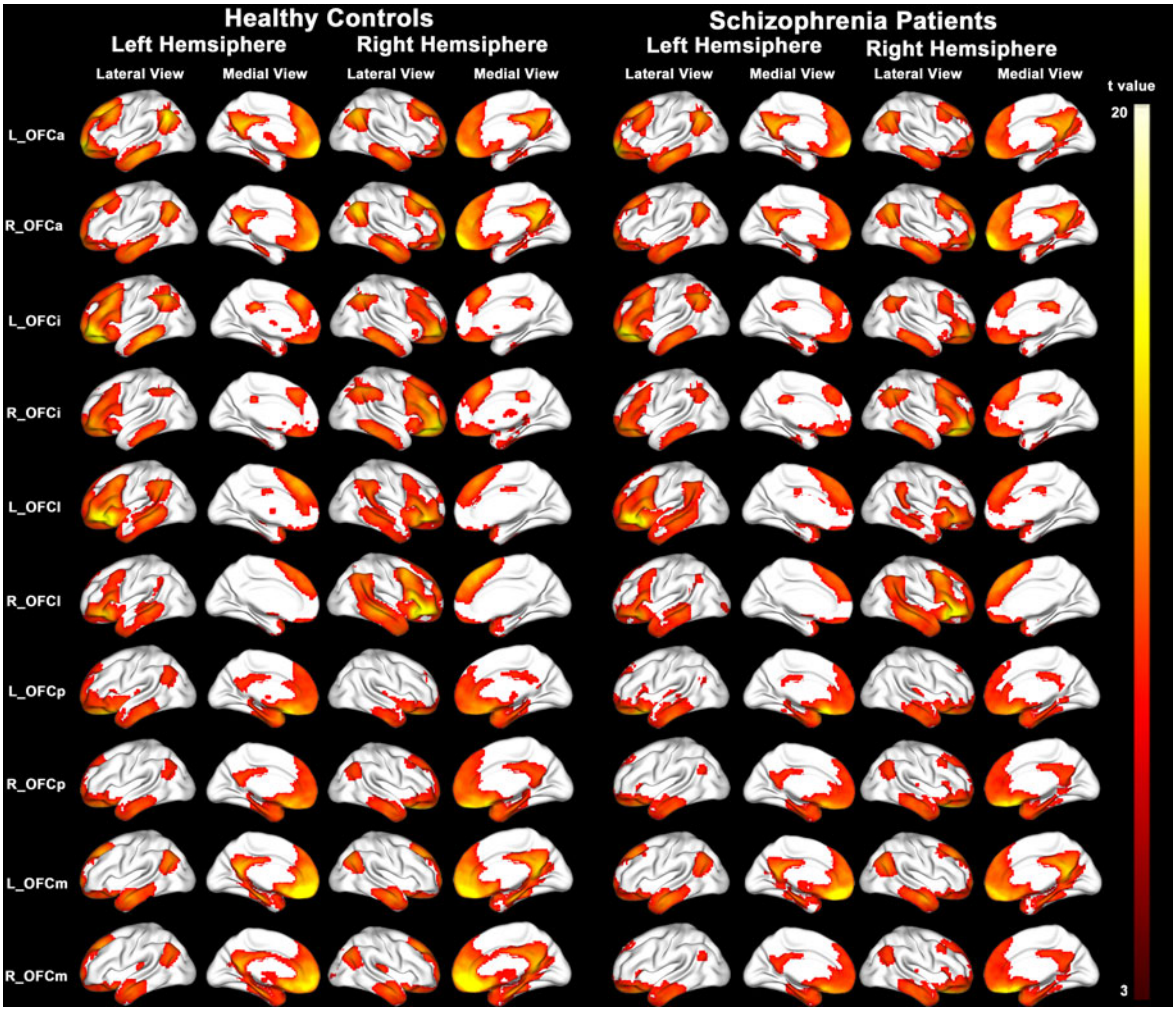


Fig. 1. The resting-state functional connectivity maps of the OFC subregions in healthy controls and schizophrenia patients. Only the positive connectivity map of each subregion is depicted ($p < 0.05/10 = 0.005$, FDR correction). L, left; R, right; OFC, orbitofrontal cortex; OFCa, anterior OFC; OFCi, intermediate OFC; OFCl, lateral OFC; OFCm, medial OFC; OFCp, posterior OFC.

we also collected fMRI data using a SENSE-SPIRAL sequence, which has been proposed to be superior to the EPI sequence in terms of imaging quality (Truong & Song, 2008). The SENSE is a parallel imaging method and has been used to shorten scan time and to reduce susceptibility-induced artifacts (Pruessmann *et al.* 1999). As expected, we found that fMRI data acquired with the SENSE-SPIRAL sequence exhibited less signal loss and distortion in the OFC regions compared with those acquired with the EPI sequence. Unfortunately, the SNR penalty is an inevitable drawback in the SENSE sequence. The SNR in SENSE images is limited by the square root of the acceleration factor. The geometry factor and *k*-space sampling patterns may also result in the decrease of SNR (Pruessmann *et al.* 1999). Hence the SENSE-SPIRAL sequence is appropriate only when the need for image quality outweighs SNR concerns. Consequently, fMRI data acquired with the SENSE-SPIRAL sequence were used for the rsFC analysis in the study.

The global signal has traditionally been thought to reflect non-neuronal noise and has been commonly regressed out during the fMRI processing. The GSR has found to improve the anatomical specificity of rsFC findings (Fox *et al.* 2009) and to enhance the detection of system-specific correlations and correspondence between resting-state correlations and anatomy (Fox *et al.* 2009). Recently, two studies have shown a huge effect of the GSR on the observed rsFC changes in schizophrenia (Yang *et al.* 2014; Wang *et al.* 2015), suggesting that global brain signal may contain neurobiological meaningful information (Scholvinck *et al.* 2010). Therefore, we performed the

https://doi.org/10.1017/S0033291717000101 Published online by Cambridge University Press

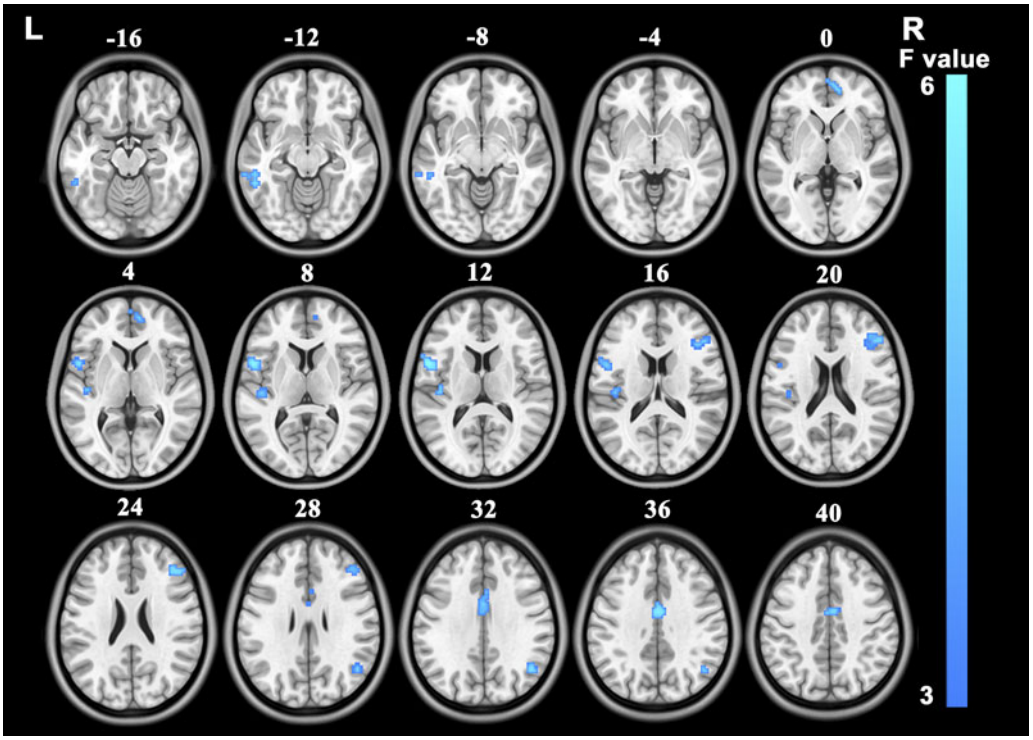


Fig. 2. Brain regions whose connectivity with OFC subregions shows significant group × subregion interaction with global signal regression (FDR corrected, $p < 0.05$). L, left; R, right.

rsFC analysis with and without GSR. Although more functional disconnections in schizophrenia were detected in data with GSR than in data without GSR, the most significant changes are highly consistent between the two preprocessing strategies. These findings suggest that the effect of the GSR is region-specific in schizophrenia. Conservatively, we only discuss the consistent findings of the rsFC analysis with and without GSR.

The GMV atrophy in multiple brain regions including the OFC has been consistently shown in schizophrenia (Baare *et al.* 1999; Herold *et al.* 2009). In consistent with these previous findings, we also found GMV atrophy in all of the OFC subregions. One may suspect that the rsFC alterations of the OFC subregions may be secondary to the GMV atrophy. To exclude this possibility, we repeated the rsFC analysis with GMV correction. We found that all the previously changed rsFCs of the OFC subregions in schizophrenia also remained significant after GMV correction, suggesting that these rsFC changes are independent of GMV atrophy.

The selective functional disconnections of the OFC subregions

We found functional disconnection between the OFCi and DLPFC in schizophrenia. As shown in Fig. 1, the OFCi was closely correlated with brain regions of the frontal-parietal network, which is composed of the DLPFC and PPC and is involved in cognitive control (Dosenbach *et al.* 2008; Zanto & Gazzaley, 2013). Thus, our finding may represent functional disconnection within the prefrontal cognitive control system, which is consistent with the functional impairment of the DLPFC in schizophrenia (Barch & Ceaser, 2012). The functional disconnection of the DLPFC has been related to executive dysfunction in schizophrenia (Su *et al.* 2013) and genetic vulnerability for schizophrenia (Woodward *et al.* 2009). Therefore, the OFCi-DLPFC functional disconnection may be associated with cognitive control impairment in schizophrenia.

The OFCi also functionally correlated with the anterolateral temporal cortex (Fig. 1), which may reflect the underlying anatomical connection of the uncinate fasciculus connecting the frontal and temporal cortices. Our finding of the functional disconnection between the OFCi and temporal cortex in schizophrenia may represent the fronto-temporal disconnection. This is in line with functional impairments in both of these regions in schizophrenia (Brown & Thompson, 2010; Guo *et al.* 2014*a*). The uncinate fasciculus has been related to cognitive abilities, such as intelligence and memory in healthy subjects (Von Der Heide *et al.* 2013). In schizophrenia, the white matter integrity reduction of the uncinate fasciculus is an

https://doi.org/10.1017/S0033291717000101 Published online by Cambridge University Press

Table 2. Post-hoc *comparisons (patients v. controls) of the resting-state functional connectivity of the orbitofrontal subregions with global signal regression*

	IFG_L		MCC		MFG_R		MTG_L		Rolandic_Oper_L		MPFC_R		AG_R	
Subregions	*t*	*p**	*t*	*p**	*t*	*p**	*t*	*p**	*t*	*p**	*t*	*p**	*t*	*p**
L_OFCa	−1.12	1.000	0.90	1.000	0.28	1.000	−2.71	0.524	0.44	1.000	−1.79	1.000	−0.74	1.000
R_OFCa	2.07	1.000	1.48	1.000	1.34	1.000	−0.99	1.000	0.68	1.000	−2.18	1.000	−3.19	0.118
L_OFCi	−2.90	0.293	1.54	1.000	−3.49	0.043	−5.60	<0.001	0.22	1.000	2.05	1.000	0.14	1.000
R_OFCi	−3.78	0.015	−0.72	1.000	−5.20	<0.001	−0.72	1.000	0.24	1.000	2.45	1.000	1.88	1.000
L_OFCl	0.35	1.000	0.20	1.000	−2.59	0.726	−2.08	1.000	−0.60	1.000	−3.70	0.020	−2.13	1.000
R_OFCl	−0.69	1.000	−2.17	1.000	−1.95	1.000	0.35	1.000	−2.22	1.000	2.91	0.289	−1.19	1.000
L_OFCm	1.19	1.000	−2.55	0.811	1.82	1.000	1.09	1.000	−1.17	1.000	−4.17	0.003	0.54	1.000
R_OFCm	−0.10	1.000	−4.23	0.003	3.05	0.185	−0.91	1.000	−4.11	0.004	−4.01	0.006	0.52	1.000
L_OFCp	−1.39	1.000	−2.85	0.342	0.20	1.000	−0.57	1.000	1.07	1.000	−2.39	1.000	0.58	1.000
R_OFCp	1.04	1.000	−2.77	0.435	0.84	1.000	−0.66	1.000	−0.03	1.000	−2.61	0.686	0.03	1.000

L, left; R, right; AG, angular gyrus; IFG, inferior frontal gyrus; MCC, middle cingulate cortex; MFG, middle frontal gyrus; MPFC, medial prefrontal cortex; MTG, middle temporal gyrus; OFC, orbitofrontal cortex; OFCa, anterior OFC; OFCi, intermediate OFC; OFCl, lateral OFC; OFCm, medial OFC; OFCp, posterior OFC; Rolandic_Oper, Rolandic operculum.
*p values are those after Bonferroni correction.

important feature (McIntosh *et al.* 2008; Wu *et al.* 2015), which may account for our finding of the fronto-temporal functional disconnection.

We also found functional disconnection between the OFCm and the posterior part of MCC (pMCC) and RO in schizophrenia. These two regions belong to the sensorimotor network and subserve sensorimotor integration and motor control. They have been found to be impaired in schizophrenia (Kim *et al.* 2010; Yu *et al.* 2011; Hammer *et al.* 2013; Guo *et al.* 2014*b*; Behroozmand *et al.* 2015). Our finding of the functional disconnection between the right OFCm and the pMCC in schizophrenia is consistent with a previous study (Wang *et al.* 2015). Thus, the functional disconnection between the right OFCm and the pMCC may represent the impairment of sensorimotor integration and motor control in schizophrenia. Besides, the RO and IFG were involved in speech production (Behroozmand *et al.* 2015). Our finding of the functional disconnection between the OFC subregions and these two regions in schizophrenia may represent the impairment of speech system.

Limitations

Several limitations in this study should be noted. First, most of these schizophrenia patients were receiving antipsychotic drug treatment, which may potentially influence on our findings, although no significant correlations were found between medication and rsFCs of the OFC in schizophrenia. Future studies with medication-naïve, first-episode schizophrenia patients are required to eliminate the medication effects and confirm the findings of this study. Second, in schizophrenia, we found changed rsFCs of the OFC subregions with multiple brain regions involved in cognitive and emotional processing. However, the lack of specific behavioral assessments may prevent us from investigating the functional relevance of these changes in schizophrenia.

Conclusion

Based on an improved imaging technique, a recently identified subregion model of the OFC, and appropriate validation approaches, we found that schizophrenia patients consistently and reliably showed functional disconnections in the bilateral OFCi and the right OFCm. These findings may not only confirm the previously proposed disconnection hypothesis of schizophrenia, but also improve our understanding of which and how OFC subregions are implicated in schizophrenia.

https://doi.org/10.1017/S0033291717000101 Published online by Cambridge University Press

Supplementary material

The supplementary material for this article can be found at https://doi.org/10.1017/S0033291717000101.

Acknowledgements

This work was supported by grants from the National Natural Science Foundation of China (81425013, 91332113 and 81271551), and Tianjin Key Technology R&D Program (14ZCZDSY00018).

Declaration of Interest

None.

References

Andreasen NC (2010). The lifetime trajectory of schizophrenia and the concept of neurodevelopment. *Dialogues in Clinical Neuroscience* **12**, 409–415.

Andreasen NC, Nopoulos P, Magnotta V, Pierson R, Ziebell S, Ho BC (2011). Progressive brain change in schizophrenia: a prospective longitudinal study of first-episode schizophrenia. *Biological Psychiatry* **70**, 672–679.

Asami T, Bouix S, Whitford TJ, Shenton ME, Salisbury DF, McCarley RW (2012). Longitudinal loss of gray matter volume in patients with first-episode schizophrenia: DARTEL automated analysis and ROI validation. *NeuroImage* **59**, 986–996.

Ashburner J. (2007). A fast diffeomorphic image registration algorithm. *NeuroImage* **38**, 95–113.

Baare WF, Hulshoff Pol HE, Hijman R, Mali WP, Viergever MA, Kahn RS (1999). Volumetric analysis of frontal lobe regions in schizophrenia: relation to cognitive function and symptomatology. *Biological Psychiatry* **45**, 1597–1605.

Baas D, Aleman A, Vink M, Ramsey NF, de Haan EH, Kahn RS (2008). Evidence of altered cortical and amygdala activation during social decision-making in schizophrenia. *NeuroImage* **40**, 719–727.

Barch DM, Ceaser A. (2012). Cognition in schizophrenia: core psychological and neural mechanisms. *Trends in Cognitive Sciences* **16**, 27–34.

Behroozmand R, Shebek R, Hansen DR, Oya H, Robin DA, Howard III MA, Greenlee JD (2015). Sensory-motor networks involved in speech production and motor control: an fMRI study. *NeuroImage* **109**, 418–428.

Brown GG, Thompson WK (2010). Functional brain imaging in schizophrenia: selected results and methods. *Current Topics in Behavioral Neurosciences* **4**, 181–214.

Chan RC, Di X, McAlonan GM, Gong QY (2011). Brain anatomical abnormalities in high-risk individuals, first-episode, and chronic schizophrenia: an activation likelihood estimation meta-analysis of illness progression. *Schizophrenia Bulletin* **37**, 177–188.

Dolan MC, Fullam RS (2009). Psychopathy and functional magnetic resonance imaging blood oxygenation level-dependent responses to emotional faces in violent patients with schizophrenia. *Biological Psychiatry* **66**, 570–577.

Dosenbach NU, Fair DA, Cohen AL, Schlaggar BL, Petersen SE (2008). A dual-networks architecture of top-down control. *Trends in Cognitive Sciences* **12**, 99–105.

Ellison-Wright I, Glahn DC, Laird AR, Thelen SM, Bullmore E (2008). The anatomy of first-episode and chronic schizophrenia: an anatomical likelihood estimation meta-analysis. *American Journal of Psychiatry* **165**, 1015–1023.

Fox MD, Zhang D, Snyder AZ, Raichle ME (2009). The global signal and observed anticorrelated resting state brain networks. *Journal of Neurophysiology* **101**, 3270–3283.

Guo Q, Tang Y, Li H, Zhang T, Li J, Sheng J, Liu D, Li C, Wang J (2014*a*). Both volumetry and functional connectivity of Heschl's gyrus are associated with auditory P300 in first episode schizophrenia. *Schizophrenia Research* **160**, 57–66.

Guo S, Kendrick KM, Yu R, Wang HL, Feng J (2014*b*). Key functional circuitry altered in schizophrenia involves parietal regions associated with sense of self. *Human Brain Mapping* **35**, 123–139.

Hammer TB, Oranje B, Skimminge A, Aggernaes B, Ebdrup BH, Glenthoj B, Baare W (2013). Structural brain correlates of sensorimotor gating in antipsychotic-naive men with first-episode schizophrenia. *Journal of Psychiatry & Neuroscience* **38**, 34–42.

Herold R, Feldmann A, Simon M, Tenyi T, Kover F, Nagy F, Varga E, Fekete S (2009). Regional gray matter reduction and theory of mind deficit in the early phase of schizophrenia: a voxel-based morphometric study. *Acta Psychiatrica Scandinavica* **119**, 199–208.

Hoptman MJ, Antonius D, Mauro CJ, Parker EM, Javitt DC (2014). Cortical thinning, functional connectivity, and mood-related impulsivity in schizophrenia: relationship to aggressive attitudes and behavior. *American Journal of Psychiatry* **171**, 939–948.

Kahnt T, Chang LJ, Park SQ, Heinzle J, Haynes JD (2012). Connectivity-based parcellation of the human orbitofrontal cortex. *Journal of Neuroscience* **32**, 6240–6250.

Kay SR, Fiszbein A, Opler LA (1987). The positive and negative syndrome scale (PANSS) for schizophrenia. *Schizophrenia Bulletin* **13**, 261–276.

Kester HM, Sevy S, Yechiam E, Burdick KE, Cervellione KL, Kumra S (2006). Decision-making impairments in adolescents with early-onset schizophrenia. *Schizophrenia Research* **85**, 113–123.

Kim DI, Sui J, Rachakonda S, White T, Manoach DS, Clark VP, Ho BC, Schulz SC, Calhoun VD (2010). Identification of imaging biomarkers in schizophrenia: a coefficient-constrained independent component analysis of the mind multi-site schizophrenia study. *Neuroinformatics* **8**, 213–229.

Kringelbach ML (2005). The human orbitofrontal cortex: linking reward to hedonic experience. *Nature Reviews Neuroscience* **6**, 691–702.

Kringelbach ML, Rolls ET (2004). The functional neuroanatomy of the human orbitofrontal cortex: evidence from neuroimaging and neuropsychology. *Progress in Neurobiology* **72**, 341–372.

https://doi.org/10.1017/S0033291717000101 Published online by Cambridge University Press

Liu F, Xie B, Wang Y, Guo W, Fouche JP, Long Z, Wang W, Chen H, Li M, Duan X, Zhang J, Qiu M, Chen H (2015*a*). Characterization of post-traumatic stress disorder using resting-state fMRI with a multi-level parametric classification approach. *Brain Topography* **28**, 221–237.

Liu F, Zhuo C, Yu C (2016). Altered cerebral blood flow covariance network in schizophrenia. *Frontiers in Neuroscience* **10**.

Liu H, Qin W, Qi H, Jiang T, Yu C (2015*b*). Parcellation of the human orbitofrontal cortex based on gray matter volume covariance. *Human Brain Mapping* **36**, 538–548.

Lynall ME, Bassett DS, Kerwin R, McKenna PJ, Kitzbichler M, Muller U, Bullmore E (2010). Functional connectivity and brain networks in schizophrenia. *Journal of Neuroscience* **30**, 9477–9487.

Mackey S, Petrides M (2010). Quantitative demonstration of comparable architectonic areas within the ventromedial and lateral orbital frontal cortex in the human and the macaque monkey brains. *European Journal of Neuroscience* **32**, 1940–1950.

Mandal MK, Pandey R, Prasad AB (1998). Facial expressions of emotions and schizophrenia: a review. *Schizophrenia Bulletin* **24**, 399–412.

McIntosh AM, Munoz Maniega S, Lymer GK, McKirdy J, Hall J, Sussmann JE, Bastin ME, Clayden JD, Johnstone EC, Lawrie SM (2008). White matter tractography in bipolar disorder and schizophrenia. *Biological Psychiatry* **64**, 1088–1092.

Mullen PE, Burgess P, Wallace C, Palmer S, Ruschena D (2000). Community care and criminal offending in schizophrenia. *Lancet* **355**, 614–617.

Naudts K, Hodgins S (2006). Schizophrenia and violence: a search for neurobiological correlates. *Current Opinion in Psychiatry* **19**, 533–538.

Ongur D, Ferry AT, Price JL (2003). Architectonic subdivision of the human orbital and medial prefrontal cortex. *Journal of Comparative Neurology* **460**, 425–449.

Pettersson-Yeo W, Allen P, Benetti S, McGuire P, Mechelli A (2011). Dysconnectivity in schizophrenia: where are we now? *Neuroscience and Biobehavioral Reviews* **35**, 1110–1124.

Power JD, Barnes KA, Snyder AZ, Schlaggar BL, Petersen SE (2013). Steps toward optimizing motion artifact removal in functional connectivity MRI; a reply to Carp. *NeuroImage* **76**, 439–441.

Pruessmann KP, Weiger M, Scheidegger MB, Boesiger P (1999). SENSE: sensitivity encoding for fast MRI. *Magnetic Resonance in Medicine* **42**, 952–962.

Pu W, Rolls ET, Guo S, Liu H, Yu Y, Xue Z, Feng J, Liu Z (2014). Altered functional connectivity links in neuroleptic-naive and neuroleptic-treated patients with schizophrenia, and their relation to symptoms including volition. *NeuroImage. Clinical* **6**, 463–474.

Sapara A, Cooke M, Fannon D, Francis A, Buchanan RW, Anilkumar AP, Barkataki I, Aasen I, Kuipers E, Kumari V (2007). Prefrontal cortex and insight in schizophrenia: a volumetric MRI study. *Schizophrenia Research* **89**, 22–34.

Scholvinck ML, Maier A, Ye FQ, Duyn JH, Leopold DA (2010). Neural basis of global resting-state fMRI activity. *Proceedings of the National Academy of Sciences USA* **107**, 10238–10243.

Shad MU, Keshavan MS, Tamminga CA, Cullum CM, David A (2007). Neurobiological underpinnings of insight deficits in schizophrenia. *International Review of Psychiatry* **19**, 437–446.

Su TW, Lan TH, Hsu TW, Biswal BB, Tsai PJ, Lin WC, Lin CP (2013). Reduced neuro-integration from the dorsolateral prefrontal cortex to the whole brain and executive dysfunction in schizophrenia patients and their relatives. *Schizophrenia Research* **148**, 50–58.

Truong TK, Song AW (2008). Single-shot dual-z-shimmed sensitivity-encoded spiral-in/out imaging for functional MRI with reduced susceptibility artifacts. *Magnetic Resonance in Medicine* **59**, 221–227.

Von Der Heide RJ, Skipper LM, Klobusicky E, Olson IR (2013). Dissecting the uncinate fasciculus: disorders, controversies and a hypothesis. *Brain* **136**, 1692–1707.

Wang D, Zhou Y, Zhuo C, Qin W, Zhu J, Liu H, Xu L, Yu C (2015). Altered functional connectivity of the cingulate subregions in schizophrenia. *Translational Psychiatry* **5**, e575.

Weissenbacher A, Kasess C, Gerstl F, Lanzenberger R, Moser E, Windischberger C (2009). Correlations and anticorrelations in resting-state functional connectivity MRI: a quantitative comparison of preprocessing strategies. *NeuroImage* **47**, 1408–1416.

Woodward ND, Waldie B, Rogers B, Tibbo P, Seres P, Purdon SE (2009). Abnormal prefrontal cortical activity and connectivity during response selection in first episode psychosis, chronic schizophrenia, and unaffected siblings of individuals with schizophrenia. *Schizophrenia Research* **109**, 182–190.

Wu L, Calhoun VD, Jung RE, Caprihan A (2015). Connectivity-based whole brain dual parcellation by group ICA reveals tract structures and decreased connectivity in schizophrenia. *Human Brain Mapping*.

Yang GJ, Murray JD, Repovs G, Cole MW, Savic A, Glasser MF, Pittenger C, Krystal JH, Wang XJ, Pearlson GD, Glahn DC, Anticevic A (2014). Altered global brain signal in schizophrenia. *Proceedings of the National Academy of Sciences USA* **111**, 7438–7443.

Yu C, Zhou Y, Liu Y, Jiang T, Dong H, Zhang Y, Walter M (2011). Functional segregation of the human cingulate cortex is confirmed by functional connectivity based neuroanatomical parcellation. *NeuroImage* **54**, 2571–2581.

Zald DH, Kim SW (1996). Anatomy and function of the orbital frontal cortex, II: function and relevance to obsessive-compulsive disorder. *Journal of Neuropsychiatry and Clinical Neurosciences* **8**, 249–261.

Zanto TP, Gazzaley A (2013). Fronto-parietal network: flexible hub of cognitive control. *Trends in Cognitive Sciences* **17**, 602–603.

https://doi.org/10.1017/S0033291717000101 Published online by Cambridge University Press